






## Article

# Comparison of Effects of Plasma Surface Modifications of Bamboo and Hemp Fibers on Mechanical Properties of Fiber-Reinforced Epoxy Composites

Pornchai Rachtanapun <sup>1,2,3,†</sup>, Choncharoen Sawangrat <sup>4,†</sup>, Thidarat Kanthiya <sup>5</sup>, Kannikar Kaewpai <sup>6</sup>, Parichat Thipchai <sup>7</sup>, Nuttapol Tanadchangsang <sup>8</sup>, Patnarin Worajittiphon <sup>2,9</sup>, Jonghwan Suhr <sup>10</sup>, Pitiwat Wattanachai <sup>11,\*</sup> and Kittisak Jantanasakulwong <sup>1,2,3,\*</sup>

<sup>1</sup> Faculty of Agro-Industry, Chiang Mai University, Chiang Mai 50100, Thailand; pornchai.r@cmu.ac.th

<sup>2</sup> Center of Excellence in Materials Science and Technology, Chiang Mai University, Chiang Mai 50200, Thailand; patnarin.w@cmu.ac.th

<sup>3</sup> Center of Excellence in Agro Bio-Circular-Green Industry, Faculty of Agro-Industry, Chiang Mai University, Chiang Mai 50100, Thailand

<sup>4</sup> Department of Industrial Engineering, Faculty of Engineering, Chiang Mai University, Chiang Mai 50200, Thailand; choncharoen@step.cmu.ac.th

<sup>5</sup> Office of Research Administration, Chiang Mai University, Chiang Mai 50200, Thailand; thidaratkanthiya05@gmail.com

<sup>6</sup> Science and Technology Park (STeP), Chiang Mai University, Chiang Mai 50100, Thailand; kannikar@step.cmu.ac.th

<sup>7</sup> Nanoscience and Nanotechnology, Faculty of Science, Chiang Mai University, Chiang Mai 50200, Thailand; parichat\_thi@cmu.ac.th

<sup>8</sup> College of Biomedical Engineering, Rangsit University, Pathumthani 12000, Thailand; nuttapol.t@rsu.ac.th

<sup>9</sup> Department of Chemistry, Faculty of Science, Chiang Mai University, Chiang Mai 50200, Thailand

<sup>10</sup> School of Mechanical Engineering, Sungkyunkwan University, Suwon-si 16419, Republic of Korea; suhr@skku.edu

<sup>11</sup> Department of Civil Engineering, Faculty of Engineering, Chiang Mai University, Chiang Mai 50200, Thailand

\* Correspondence: pitiwat@step.cmu.ac.th (P.W.); kittisak.jan@cmu.ac.th (K.J.); Tel.: +66-(0)53948274 (P.W. & K.J.); Fax: +66-(0)53948230 (P.W. & K.J.)

† These authors contributed equally to this work.



**Citation:** Rachtanapun, P.; Sawangrat, C.; Kanthiya, T.; Kaewpai, K.; Thipchai, P.; Tanadchangsang, N.; Worajittiphon, P.; Suhr, J.; Wattanachai, P.; Jantanasakulwong, K. Comparison of Effects of Plasma Surface Modifications of Bamboo and Hemp Fibers on Mechanical Properties of Fiber-Reinforced Epoxy Composites. *Polymers* **2024**, *16*, 3394. <https://doi.org/10.3390/polym16233394>

Academic Editor: Ming Zhang

Received: 7 November 2024

Revised: 25 November 2024

Accepted: 27 November 2024

Published: 30 November 2024



**Copyright:** © 2024 by the authors. Licensee MDPI, Basel, Switzerland. This article is an open access article distributed under the terms and conditions of the Creative Commons Attribution (CC BY) license (<https://creativecommons.org/licenses/by/4.0/>).

**Abstract:** In this study, we investigated the behaviors of epoxy composites reinforced with bamboo (BF) and hemp (HF) fibers. Both fibers were treated using dielectric barrier discharge (DBD) plasma for various durations (2.5 to 20 min). Epoxy resin (ER) was mixed with BF or HF with and without plasma treatment. The Fourier-transform infrared spectra of the plasma-treated fibers showed an enhanced peak intensity of carboxyl groups. ER/BF treated for 20 min exhibited a high tensile strength (up to 56.5 MPa), while ER/HF treated for 20 min exhibited a more significant increase in elongation at break (6.4%). Flexural tests indicated that the plasma treatment significantly improved the flexural strength of the hemp composites (up to 62.2 MPa) compared to the bamboo composites. The plasma treatment increased the fiber surface roughness and interfacial bonding in both composites. The thermal stability and wettability were improved by the DBD plasma treatment. The DBD plasma treatment enhanced the interfacial adhesion between fibers and ER matrix, which improved the mechanical, thermal, and wettability properties of the composites.

**Keywords:** plasma; surface modification; bamboo; hemp; epoxy composites

## 1. Introduction

In recent years, biocomposites have emerged as versatile materials in various industries [1,2]. They are environmentally friendly material alternatives for the replacement of petroleum-based polymers due to their ability to combine the strengths of polymers with reinforcing materials. The reinforced polymers by biomaterials exhibit enhanced mechanical,

thermal, and chemical properties. Composites are produced by embedding a reinforcing phase within a polymer matrix [3], which provides lightweight structures, strength, and durability. The use of cellulose fibers, such as bamboo, flax, sisal, jute, and kenaf, in polymer composites as reinforcement gained popularity in several engineering applications due to the low cost, density, favorable mechanical properties, and recyclability [4,5]. Cellulose fibers are environmentally friendly, nontoxic, and renewable materials. Manufacturing industries, such as the packaging, building construction, automotive, and furniture industries, have been encouraged to use plant fibers instead of reinforcing materials [6–8].

Natural fibers are a biomaterial used to reinforce a polymer matrix. Bamboo belongs to the grass family poaceae, which is known for its strength and ability to thrive in diverse climates [9]. Bamboo is composed of a series of nodes and internodes, which yields a hollow cylindrical structure. The cellulose and lignin contents of bamboo fibers are up to 40–50% and 20–30%, respectively, which provides rigidity, high tensile strength, and high stiffness [10,11]. This composition makes bamboo a strong and flexible material, which can be used for various construction and industrial applications. In the context of fiber reinforcement, bamboo is processed into bamboo fibers (BFs) for use in polymer composites. These fibers exhibit a high tensile strength, comparable to those of some synthetic fibers [12,13]. Bamboo fiber composites are increasingly used in construction, automotive components, and packaging due to their lightweight structure, strength, and biodegradability. Hemp is another natural alternative for composite reinforcement. Hemp fibers (HFs) are strong and lightweight, and exhibit favorable thermal properties, making them ideal for composites requiring enhanced toughness and thermal stability. HF contains cellulose (60–70%), hemicellulose (15–25%), and lignin (5–10%), which provides excellent mechanical properties. Hemp has been used in textiles for centuries. Its potential as a reinforcing fiber in polymer composites is particularly recognized in sustainable manufacturing sectors [14,15]. However, the hydrophilic property of plant fibers, hydrophobic property of resins, and compatibility problems limit the application of composites [16]. Surface treatments with chemical and physical methods are employed to enhance the interfacial adhesion between natural fibers and matrix resins. Substantial studies have been carried out to improve interfacial adhesion by chemical, physical, or other modification methods. Common surface modification methods include alkali, silane, plasma, and enzymatic treatments [17–21]. These treatments improve the fiber surface by increasing the roughness or introducing functional groups that enhance the adhesion, which leads to transfer load between the fiber and matrix [22,23]. Natural fiber composites are increasingly used in construction, automotive components, and packaging [24,25] due to their lightweight structure, strength, and biodegradability.

Plasma treatment involves exposure of a material surface to a partially ionized gas (plasma), electrons, ions, and neutral particles. The interaction between the plasma and surface induces chemical, physical, and structural modifications of materials [26]. The use of dielectric barrier discharge (DBD) plasma is a specific form of atmospheric plasma treatment with a dielectric barrier that separates two electrodes. This setup provides uniformity of nonthermal plasma generation at atmospheric pressure. The DBD plasma is frequently used to treat natural fibers due to its energy efficiency and scalability. In the DBD plasma, various gasses can be used, such as O<sub>2</sub>, N<sub>2</sub>, or Ar, depending on the desired surface modification [27–29]. Natural fiber surface improvement by DBD plasma is a novel process to increase roughness and reactive functional groups on fiber surface to form physical and chemical crosslinking with the polymer matrix, respectively. The synergistic crosslinking power may increase properties of polymer composite which can be applied for construction, electrical, coating, packaging, agriculture, and medical applications.

Epoxy resin (ER) is the most used thermoset structure in engineering fields owing to its chemical resistance, excellent mechanical properties, and electrical insulation [30]. ERs are created through reactions between epoxides (three-membered cyclic ethers) and curing agents (hardener agents), such as amines, anhydrides, or phenols. Upon curing, epoxy forms a rigid crosslinked network structure that provides the characteristic strength and

durability [31]. Fiber-reinforced epoxy composite is a material obtained by embedding high-strength fibers into an ER matrix. This combination creates a composite material with superior mechanical properties compared to those of the individual components. The fibers act as a reinforcing material to provide strength and stiffness, while the ER acts as a matrix that binds the fibers together, distributes stress, and protects the fibers from damage [32,33]. Some researchers attempted to develop natural fiber-reinforced ERs without surface modification, which led to weak mechanical properties and connecting phase between fibers and the ER matrix. The use of chemical and physical processes is a target approach to improve the fiber surface before blending with ER. When the surface of the fiber is improved by chemical and physical roughness, this improves the reaction, interfacial adhesion, and properties of the blend.

Therefore, in this study, a combined surface modification, with chemical and physical processes, by the plasma technology was used to improve the surface of BF and HF. BF and HF were plasma-treated using an argon + oxygen gas (Ar + O<sub>2</sub>) for different times of 0 to 20 min, followed by plating in an NH<sub>4</sub>OH solution to improve the chemical structure of the fibers. NH<sub>4</sub>OH was used to provide grafting –NH<sub>2</sub> groups onto the surface structure of the fibers, which can react with epoxy groups of ER. The DBD plasma technique was used to improve the roughness surface and polarity of the fibers. The properties of both fiber composites were investigated. Fourier-transform infrared (FTIR) spectroscopy was utilized to evaluate the chemical bonding and reaction mechanisms within the composites, while tensile strength and flexural properties were evaluated to assess the impact of the plasma treatment. Morphological and thermal stability studies were carried out to explain the impact of the plasma treatment on the composite structure and performance. This research provides insights into the potential of plasma-treated natural fiber composites in creating stronger and more durable ecofriendly materials for industrial applications.

## 2. Materials and Methods

### 2.1. Materials

BFs were obtained from South Samoeng, Chiang Mai, Thailand. HFs were purchased from Royal Project Foundation, Chiang Mai, Thailand. ER was of grade A302. A hardener of grade A301 was purchased from Easy Resin, Co., Ltd., Nonthaburi, Thailand. All chemicals for the surface modification, including sodium hydroxide (NaOH), sodium chlorite (NaClO<sub>2</sub>), and ammonium hydroxide (NH<sub>4</sub>OH), were purchased from Merck & Co. Inc., Darmstadt, Germany.

### 2.2. Surface Treatment of Fibers

Before the plasma treatment, bamboo and hemp fibers were mildly alkaline treated in an aqueous NaOH solution (20% *w/v*) at 80 °C for 5 h. The pulps were bleached with NaClO<sub>2</sub> to remove lignin and hemicellulose, as described in our previous report [28]. The fibers were sieved through a 180 μm sieve. The bamboo and hemp fibers were treated for surface modification using a DBD plasma approach. The DBD plasma machine is shown in Figure 1. The fibers were put on the tray, while DBD was generated through two parallel high-power electrodes covered by a thin quartz foil. The grounded electrode can be adjusted to change the discharge gap for the fibers. The DBD plasma was generated by a high-voltage power of 180 W (3.45 W/cm<sup>2</sup>) with a constant frequency of 13.56 kHz. Ar + O<sub>2</sub> gasses were used for plasma flow rates of 8 and 10 L/min, respectively. The DBD plasma was applied on the bamboo and hemp fibers for 2.5, 5, 10, 15, and 20 min. The treated fibers under each plasma condition were modified on the surface by mixing into an NH<sub>4</sub>OH solution (1:10% *w/v*). The sample was heated by a hot plate at 60 °C and stirred continuously for 1 h. Afterward, the NH<sub>4</sub>OH solution was evaporated from the final product by heating at 60 ± 2 °C for 48 h.



**Figure 1.** Dielectric barrier discharge (DBD) plasma machine.

### 2.3. Fiber Composite Material Fabrication

The fiber composite materials were fabricated by the hand layup technique followed by the mixing of ER and hardener (2:1%  $w/w$ ), as indicated in Table 1. The fiber composites were separated into untreated ( $F_{untr}$ ) and treated ( $F_{tr}$ ) plasma groups for the different natural fiber types (bamboo and hemp), and then the fiber samples were mixed with ER at room temperature. The mixed samples were stirred to enhance the dispersion of fibers, while air bubbles were removed in the ER with an aspirated vacuum. The mixture was then cast into a silicone mold of a bone shape followed by drying at 80 °C for 5 h.

**Table 1.** Notation of the composite material samples (%  $w/w$ ).

Sample	Type of Fiber		Epoxy:Hardener (2:1)	Fiber
	Bamboo	Hemp	(%)	(%)
ER/BF <sub>untr</sub>	✓		95	5
ER/BF <sub>tr</sub> 2.5	✓		95	5
ER/BF <sub>tr</sub> 5	✓		95	5
ER/BF <sub>tr</sub> 10	✓		95	5
ER/BF <sub>tr</sub> 15	✓		95	5
ER/BF <sub>tr</sub> 20	✓		95	5
ER/HF <sub>untr</sub>		✓	95	5
ER/HF <sub>tr</sub> 2.5		✓	95	5
ER/HF <sub>tr</sub> 5		✓	95	5
ER/HF <sub>tr</sub> 10		✓	95	5
ER/HF <sub>tr</sub> 15		✓	95	5
ER/HF <sub>tr</sub> 20		✓	95	5

### 2.4. FTIR Spectroscopy

The chemical functional groups of the samples were examined using FTIR spectroscopy (Thermo Nicolet 6700 FTIR spectrometer, Thermo Fisher Scientific, Woodland, CA, USA) with the ATR mode. FTIR spectra were acquired in the range of 500–4000  $cm^{-1}$  (32 scans, scan resolution of 4  $cm^{-1}$ ).

### 2.5. Tensile Properties

The bone-shaped configuration samples were prepared with dimensions of 2 mm × 5 mm × 1 mm (width × length × thickness). The test was carried out according

to the JISK-6251-7 standard (Model MCT1150, Tokyo, Japan) at room temperature. The elongation at break (EB) and tensile strength (TS) were measured at a crosshead speed of 50 mm/min. Ten replicates were performed on each sample.

### 2.6. Flexural Test

The samples were cast into the silicone mold with dimensions of 13 mm × 65 mm × 3 mm (width × length × thickness) according to the American Society for Testing and Materials (ASTM) D790 standard. The testing was conducted using a universal testing machine (H1KS, Hounsfield Test Co., Ltd., Surrey, UK) in a three-point bending configuration with a force of 1 kN at room temperature. The average from five samples was recorded for the analysis. The flexural strength and modulus were calculated by the following [28]:

$$\text{Flexural strength} = \frac{3FL}{2bd^2}, \quad (1)$$

$$\text{Flexural modulus} = \frac{mL^3}{4bd^3} \quad (2)$$

where  $F$ ,  $L$ ,  $b$ ,  $d$ , and  $m$  are the maximum failure load (N), length of span (mm), width, thickness, and slope of the load–displacement curve tangent to the initial line, respectively.

### 2.7. Morphological Analysis

The fractured morphologies of the samples were studied by scanning electron microscopy (SEM; JSM-IT300LV, JEOL Co., Ltd., Tokyo, Japan). The impact fracture surface broken in liquid nitrogen was evaporated in a hot air oven at 60 °C for 2 h. The samples were sputter-coated with gold and observed at 15 kV under a vacuum.

### 2.8. Thermal Stability

The thermal stabilities of the epoxy and fiber-reinforced epoxy composites were evaluated by a thermogravimetric analysis (TGA; Mettler Toledo STARe TGA/DSC3+, Greifensee, Switzerland) under a nitrogen atmosphere. The testing temperature range was 25–600 °C, while the rate was 10 °C/min.

### 2.9. Contact Angle

The water contact angle was measured using a water droplet instrument (DSA30E, Krüss Co., Ltd., Hamburg, Germany). Samples were formed by casting them into a silicone mold and pasting them on glass slides. The water drop shape was recorded at 0–10 min. At least five measurements of each sample were performed to average the water contact angles.

### 2.10. Statistical Analysis

A statistical comparison was carried out using a one-way analysis of variance (ANOVA) with the SPSS software (SPSS version 17, Armonk, NY, USA). The statistical significance ( $p < 0.05$ ) was estimated using the Duncan test.

## 3. Results and Discussion

### 3.1. FTIR Spectroscopy

The chemical characteristics of the fiber-reinforced epoxy composites evaluated by FTIR spectroscopy for bamboo and hemp fibers with DBD plasma treatment are shown in Figure 2. The untreated and treated fibers exhibited hydroxyl (O–H) stretching vibrations at 3330 to 3400  $\text{cm}^{-1}$  [34,35]. The band at 2890  $\text{cm}^{-1}$  was assigned to the C–H stretching vibration of the cellulose fiber containing a functional group of alkanes [36], while the band at 1635  $\text{cm}^{-1}$  was attributed to the aromatic of lignin [37,38]. The peak around 1730  $\text{cm}^{-1}$  was indicated to the carbonyl (C=O) stretching of acetyl groups of hemicellulose [39]. Both plasma-treated and untreated fibers exhibited peak disappearance of lignin at 1635  $\text{cm}^{-1}$  partly due to the alkaline treatment and bleaching before the

plasma treatment. In the ER/BF and ER/HF composites, ER exhibited C–C stretching peaks at 1610 and 1585  $\text{cm}^{-1}$  and C=C stretching vibrations of the ER aromatic ring at 1508 and 1454  $\text{cm}^{-1}$  [40]. The bands at 1241, 913, and 827  $\text{cm}^{-1}$  were C–O symmetrical stretching, C–O asymmetrical stretching, and C–O–C stretching in the oxirane ring, respectively [41,42]. For the plasma-treated composites, an increase in peak intensity at 3200–3600  $\text{cm}^{-1}$  was observed due to O–H stretching of hydroxyl groups of the fibers. The treatment with the Ar + O<sub>2</sub> gas generated the polar groups of carbonyls (C=O) and carboxyl (–COOH) at 1680–1720  $\text{cm}^{-1}$ . In addition, carbon hydrogen group (CH<sub>2</sub>, CH<sub>3</sub>) stretching was observed at 2850–3000  $\text{cm}^{-1}$  [28,43]. The amount of oxygen-containing groups on the surface increased with the time of plasma treatment owing to bonding between the fiber and resin [44]. However, the epoxy groups of ER (912  $\text{cm}^{-1}$ ) were not observed on the ER/BF<sub>tr</sub> composite (Figure 2a). The ER/BF<sub>tr</sub> composites exhibited a new shoulder peak at 1700  $\text{cm}^{-1}$ , which disappeared upon the treatment for 20 min. This new peak indicates a new C–O formation from the reaction between the ER and BF surface, which changed the form with the 20 min treatment. HF<sub>untr</sub> exhibited –COOH at 1730  $\text{cm}^{-1}$  and C–O at 1360  $\text{cm}^{-1}$ . The intensities of these two peaks increased with the plasma treatment due to the increasing contents of the –COOH and C–O groups on the surface of HF. The results indicate that the –COOH groups react with NH<sub>4</sub>OH and epoxy groups of ER. –COOH groups disappeared after mixing with ER. The results also indicate that –NH<sub>2</sub> groups graft on the fiber surface and react with epoxy groups of ER. For the ER/HF composites, the intensity of epoxy groups of ER at 912  $\text{cm}^{-1}$  decreased with the time of plasma treatment owing to the high reaction rate between the surface of HF and ER. The plasma treatment improves the reactive functional groups of the fibers surface, which react with epoxy groups of the ER main matrix [10,42,45]. The plasma treatment caused changes in the chemical and physical structures of the bamboo and hemp fibers [27,46,47], resulting in the formation of functional groups that induced bonds and interfacial adhesion between EB matrix and the fiber. These reactions could improve the properties of composites.

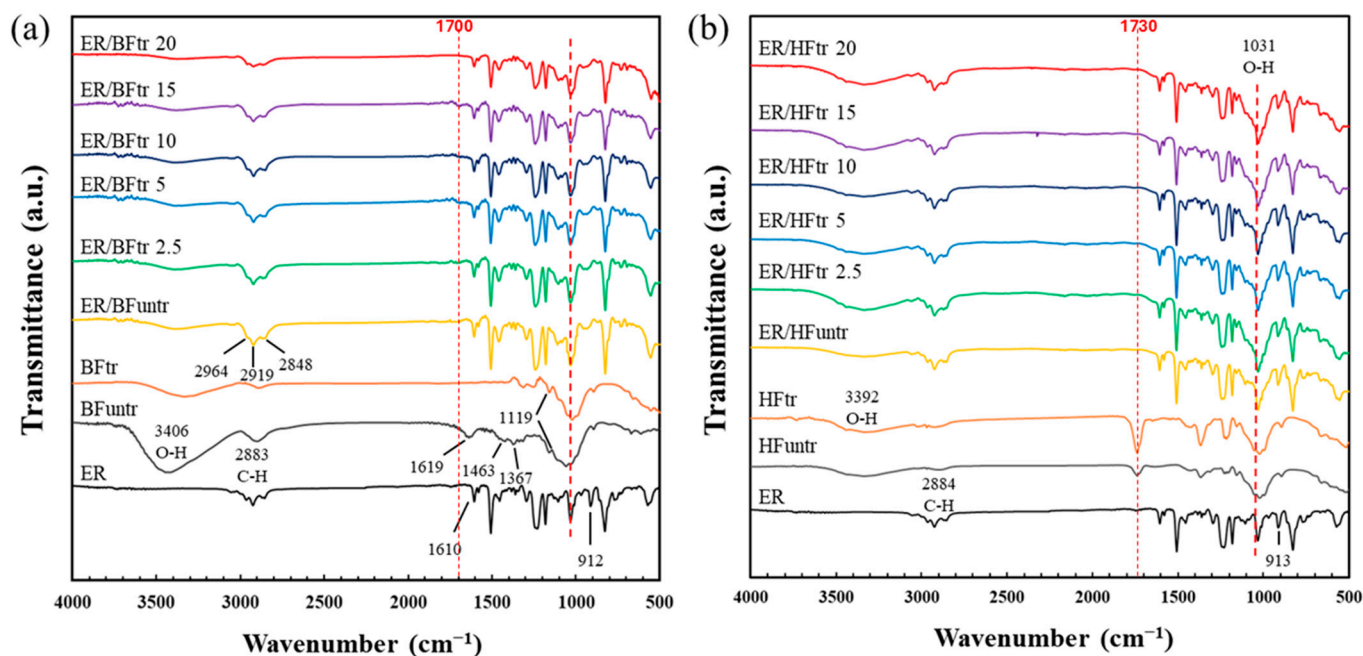


**Figure 2.** FTIR spectra of (a) bamboo and (b) hemp fiber-reinforced epoxy composites (untreated and treated with Ar + O<sub>2</sub> for 2.5–20 min + NH<sub>4</sub>OH).

### 3.2. Tensile Properties

Figure 3 shows the tensile properties of ER composites with plasma treatment (0–20 min) on BF and HF. The tensile strength and elongation at break of the ER/BF<sub>untr</sub>

composite using bamboo untreated fibers were 42 MPa and 4.7%, respectively. The EP/BF<sub>tr</sub> composites treated bamboo with the Ar + O<sub>2</sub> gas for 2.5–20 min exhibited increasing tensile strength and elongation at break with the treatment time. They exhibited the highest tensile strength at 20 min (56.5 MPa). The tensile strength and elongation at break of the hemp untreated composite (ER/HF<sub>untr</sub>) were 43.4 MPa and 3.6%, respectively. The EP/HF<sub>tr</sub> composites exhibited higher tensile strengths than that of the untreated composite (highest value of 53.2 MPa at 5 min), which slightly decreased with the increase in treatment time. The elongation at break of the EP/HF<sub>tr</sub> composite significantly increased with the treatment time from 3.6% to 6.4%. The improved tensile properties of the bamboo and hemp fiber-reinforced epoxy composites were attributed to the adhesion between the fibers and ER matrix. The plasma treatment of the fibers significantly affected the adhesion performance of the interface between the reinforced fibers and ER [48]. The samples using the hemp-treated fiber reinforcement were improved in terms of elongation at break, while the bamboo-treated fibers provided a larger improvement in tensile strength. The surface roughness of the fibers increased due to plasma etching, which enhanced the penetration and diffusion at the fiber–matrix interface and generated interlocking bonds [27,49]. The high degree of interfacial chemical reaction between epoxy groups of ER and –COOH groups of fibers with physical crosslinking with a high fiber roughness could improve the mechanical properties of the composites. Optimal plasma processing parameters relate to mechanical properties of the composites [50].

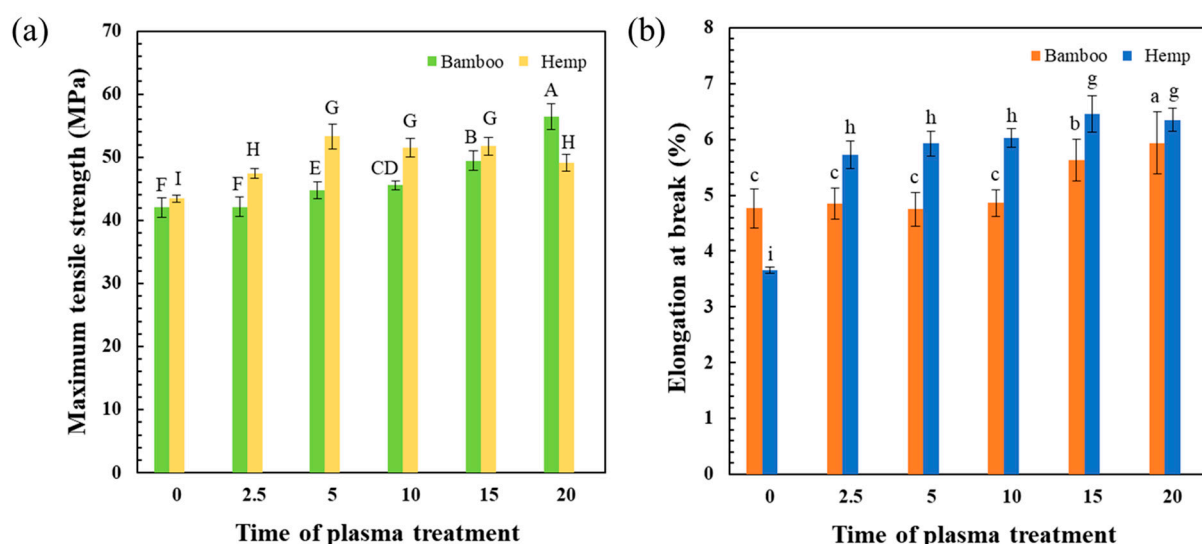


**Figure 3.** Comparison of tensile properties between bamboo and hemp fiber-reinforced epoxy composites, untreated (0) and treated with Ar + O<sub>2</sub> for 2.5–20 min + NH<sub>4</sub>OH. (a) Maximum tensile strength (MPa) and (b) elongation at break (%). The mean values of the tensile strength (uppercase letter) and elongation at break (lowercase letter) differ significantly ( $p < 0.05$ ).

### 3.3. Flexural Test

We evaluated the flexural strengths of the composites according to the plasma treatment of the bamboo and hemp fibers, as shown in Table 2. The flexural strength and modulus of the bamboo untreated composite (ER/BF<sub>untr</sub>) were 55.9 MPa and 7.6 GPa, respectively. The flexural strengths of ER/BF<sub>tr</sub> treated for 2.5, 5, 10, 15, and 20 min were 54.8, 50.5, 56.8, 58.1, and 57.5 MPa, while the flexural moduli were 6.9, 6.6, 8.2, 8.1, and 7.7 GPa, respectively. The ER/HF<sub>untr</sub> composite exhibited a flexural strength and modulus of 54.7 MPa and 7.6 GPa, respectively. The flexural strengths (53.9, 47.9, 56.7, 54.4, and 62.2 MPa) and moduli (7.7, 6.7, 7.8, 7.5, and 8.6 GPa) of the hemp fiber-reinforced composites after the plasma treatment exhibited increasing trends with the treatment time due to the improvements in HF<sub>tr</sub> roughness and interfacial adhesion of the ER/HF<sub>tr</sub> composites. The DBD plasma treatment with O<sub>2</sub> gas improved the mechanical properties of both bam-

boo and hemp [51]. Both flexural stress and modulus of hemp were significantly improved compared to those of bamboo due to the different chemical structure of the hemp fibers with a responsive structural basis to the plasma treatment compared to the bamboo [52,53].

**Table 2.** Comparison of flexural strengths and flexural moduli of the composites with untreated and plasma-treated fibers.

Sample	Bamboo (B)		Hemp (H)	
	Flexural Stress (MPa)	Flexural Modulus (GPa)	Flexural Stress (MPa)	Flexural Modulus (GPa)
ER/F <sub>untr</sub>	55.9 ± 4.6 <sup>BC</sup>	7.6 ± 0.6 <sup>ab</sup>	54.7 ± 0.8 <sup>I</sup>	7.6 ± 0.1 <sup>j</sup>
ER/F <sub>tr</sub> 2.5	54.8 ± 6.8 <sup>AB</sup>	6.9 ± 0.5 <sup>bc</sup>	53.9 ± 0.7 <sup>I</sup>	7.7 ± 0.1 <sup>i</sup>
ER/F <sub>tr</sub> 5	50.5 ± 7.8 <sup>A</sup>	6.6 ± 0.3 <sup>c</sup>	47.9 ± 0.8 <sup>J</sup>	6.7 ± 0.1 <sup>k</sup>
ER/F <sub>tr</sub> 10	56.8 ± 5.1 <sup>C</sup>	8.2 ± 0.7 <sup>a</sup>	56.7 ± 0.9 <sup>H</sup>	7.8 ± 0.1 <sup>i</sup>
ER/F <sub>tr</sub> 15	58.1 ± 5.4 <sup>C</sup>	8.1 ± 0.7 <sup>a</sup>	54.4 ± 1.6 <sup>I</sup>	7.5 ± 0.2 <sup>j</sup>
ER/F <sub>tr</sub> 20	57.5 ± 5.9 <sup>C</sup>	7.7 ± 0.8 <sup>ab</sup>	62.2 ± 1.1 <sup>G</sup>	8.6 ± 0.2 <sup>h</sup>

Significantly different mean values of the flexural stress (uppercase letter) and flexural strain (lowercase letter) ( $p < 0.05$ ).

### 3.4. Morphological Analysis

SEM was employed to acquire fractured surface images of the composites. Figure 4 shows the morphologies of the fiber-reinforced epoxy composites with bamboo and hemp structures, untreated and plasma-treated for different times. The ER/BF<sub>untr</sub> composite with the untreated fibers exhibited a smooth surface of the bamboo fiber similar to that of the ER/BF<sub>tr</sub> 2.5 sample. The increase in the time of plasma treatment (5–20 min) resulted in a high fiber roughness due to the oxygen in the discharge gasses inducing oxygen groups onto the fiber structure. The plasma treatment induces etching and formation of chemical species on the surface, which corresponds to the roughness [54]. Fine BF<sub>tr</sub> and HF<sub>tr</sub> fibers distribution on ER matrix were observed, which provided the properties improvement of composite [55,56]. The bamboo fiber-reinforced composites exhibited obvious gaps between fibers and matrix due to the plasma treatment with O<sub>2</sub> gas resulting in surface etching and reducing the polarity of the fiber by the formation of oxygen bonding [28,57,58]. Reduction in gaps between the BF surface and ER matrix were observed for the plasma treatment of 20 min, which related to the increased tensile strength. However, ER/HF<sub>tr</sub>20 showed low gaps between HF and ER matrix with reduction in tensile strength due to the occurred degradation of HF fiber which was weaker structure than BF fiber. Combination between interfacial crosslinking and fiber degradation provided slightly decreased tensile strength. The SEM images of the HF-reinforced composites showed different characteristics from those of the bamboo fibers. The morphology of the ER/HF<sub>untr</sub> composite with untreated fibers clearly exhibited hemp stem sections [59] with characteristics of smooth fibers, large pores, and irregular structure [22,52]. The EP/HF<sub>tr</sub> composites exhibited low gaps between the HF and BR matrix for all treatment times owing to the high interfacial adhesion between HF and BR via chemical and physical HF surface improvements. The ER/HF<sub>tr</sub> composites exhibited surface improvements without removed fibers due to the excellent adhesion between the HF and EP [28,60]. The DBD plasma affected the etching of the fiber surface, enhanced the roughness, and induced –COOH groups on the HF structure, due to the surface ion bombardment, etching, and ablation of surface layers [61]. Long-term treatment provided crosslinking reaction which improved interfacial adhesion and mechanical properties of the composites.

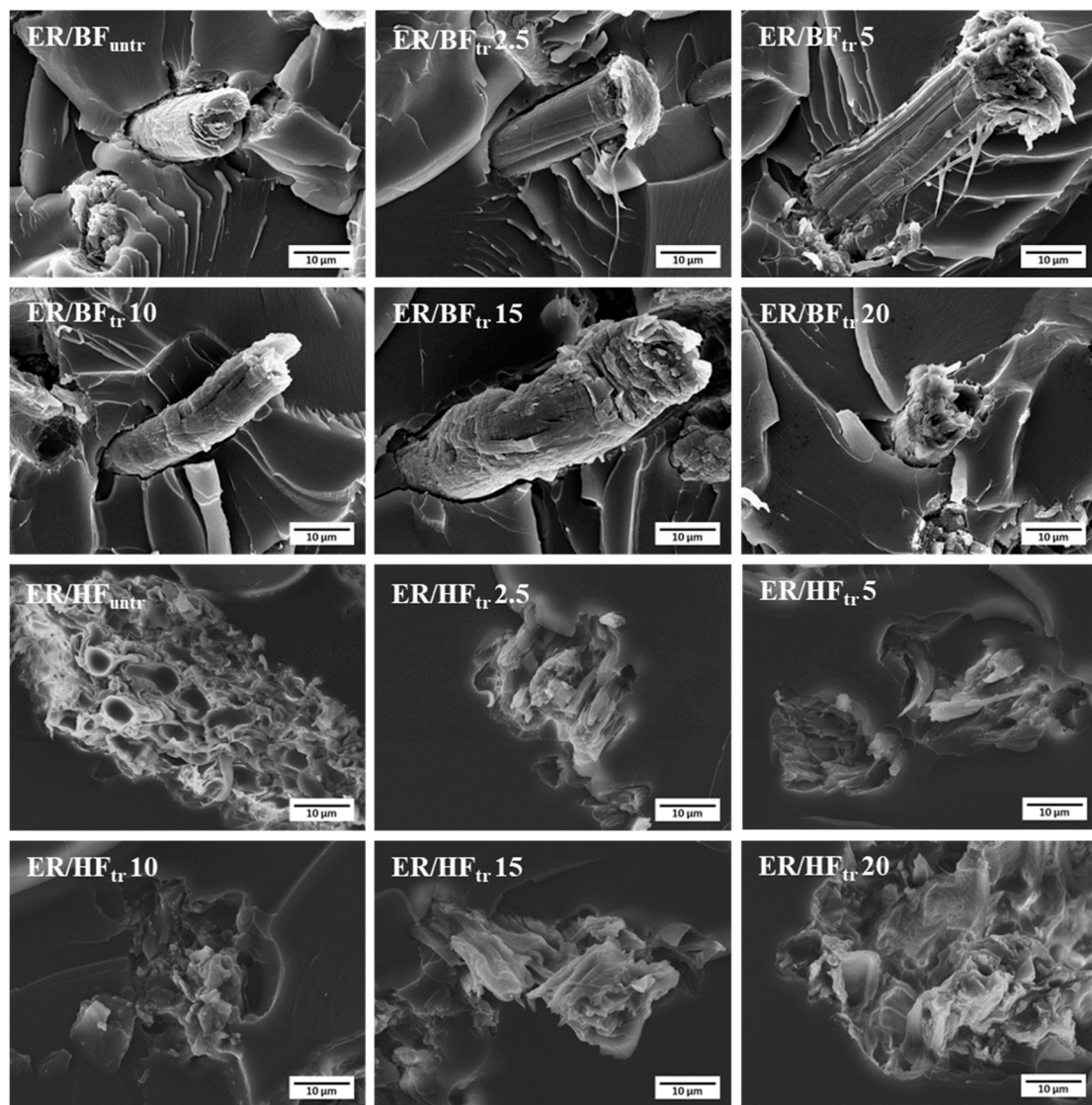


**Figure 4.** SEM images of BF- and HF-reinforced epoxy composites, untreated and treated with Ar + O<sub>2</sub> gas for different times at 1000 $\times$ .

### 3.5. Thermal Stability

The results of the thermal analysis of the pure epoxy and fiber-reinforced ER composites with untreated fibers and plasma-treated fibers with Ar + O<sub>2</sub> gas for different times are shown in Figure 5. Weight loss of the epoxy is observed in the first stage at approximately 150 °C due to the released humidity of the composites [62,63]. The ER/BF and ER/HF composites exhibited similar behaviors with the treatment time. In the temperature range of 200–350 °C, the ER blend with fibers exhibited a higher weight loss than the pure ER, which increased with the treatment time. All composites exhibited fiber degradation at 370 °C owing to the degradation of cellulose and hemicellulose composition in the fibers [64]. The phase of lignin was decomposed in the range of 400 to 460 °C with a weight loss percentage of 6%. A higher temperature is needed to decompose hemicellulose, cellulose, and lignin. The remaining component at 500 to 600 °C had an ash content, increasing with the treatment time due to the high degree of crosslinking reaction around the interface of the fibers with ER [65]. The crosslinking improved the interfacial adhesion and mechanical properties of the composites.

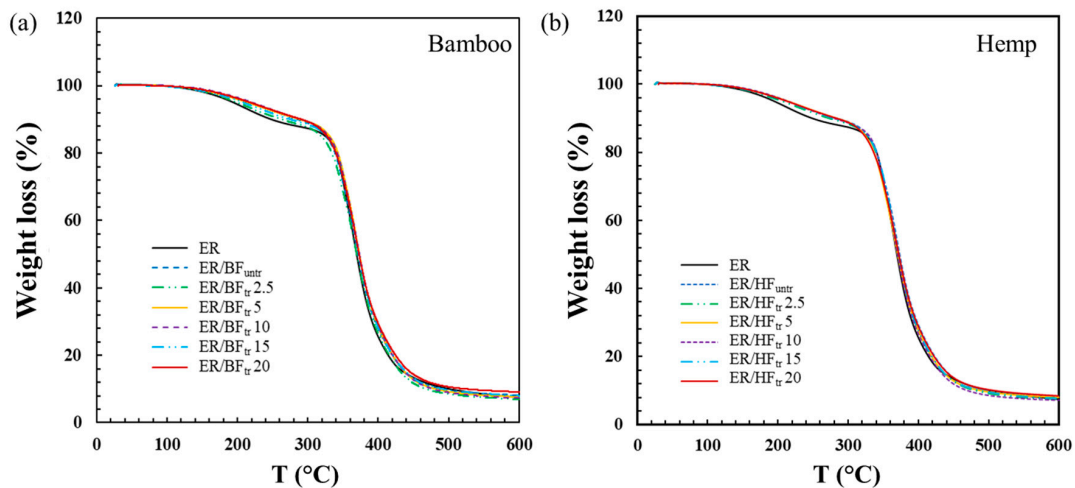


**Figure 5.** TGA curves of (a) BF- and (b) HF-reinforced epoxy composites with untreated fibers and fibers treated with Ar + O<sub>2</sub> gas for different times.

### 3.6. Water Contact Angle

The wettability properties of the composites were calculated using a contact angle measurement, as shown in Figure 6. Water droplets were dropped onto the composite surfaces and automatically recorded from 0 to 10 min. The untreated BF composite (EP/BF<sub>untr</sub>) exhibited a contact angle of 72° after 10 min (Figure 6a), which implies a low surface wettability. The treated samples exhibited decreased water contact angles after 10 min with the increase in treatment time (65, 62, 62, and 57°) due to the high polarity of the plasma treatment, which increased with the 20 min treatment (67°) because of the high crosslinking degree and surface roughness effect of BF<sub>tr</sub>. The ER/HF<sub>untr</sub> composite exhibited a contact angle of 85° after 10 min (Figure 6b), which decreased with the enhance in the plasma treatment time (82, 82, 83, 81, 77°). The decreasing water droplet contact angle of ER/HF<sub>tr</sub> indicates a high amount of generated –COOH and –OH groups on the HF<sub>tr</sub> structure, which reduced the contact angle by its hydrophilicity. However, for BR/BF<sub>tr</sub> treated for 20 min, the contact angle was increased due to the high crosslinking density between the BF<sub>tr</sub> and ER matrix. Crosslinking reaction and the enhanced crosslinking amount with time treatment were confirmed by FTIR and TGA results, respectively. Both composite fibers exhibited decreasing contact angles with the increase in the DBD plasma treatment time due to the increases in the surface roughness, porosity, and amount of hydrophilic groups of the fibers subjected to the Ar + O<sub>2</sub> gas treatment, which led to etching of the surface fibers [48,66]. The long-term plasma treatment affected the water penetration into the fibers and decreased the water resistance of the composite [28,67].

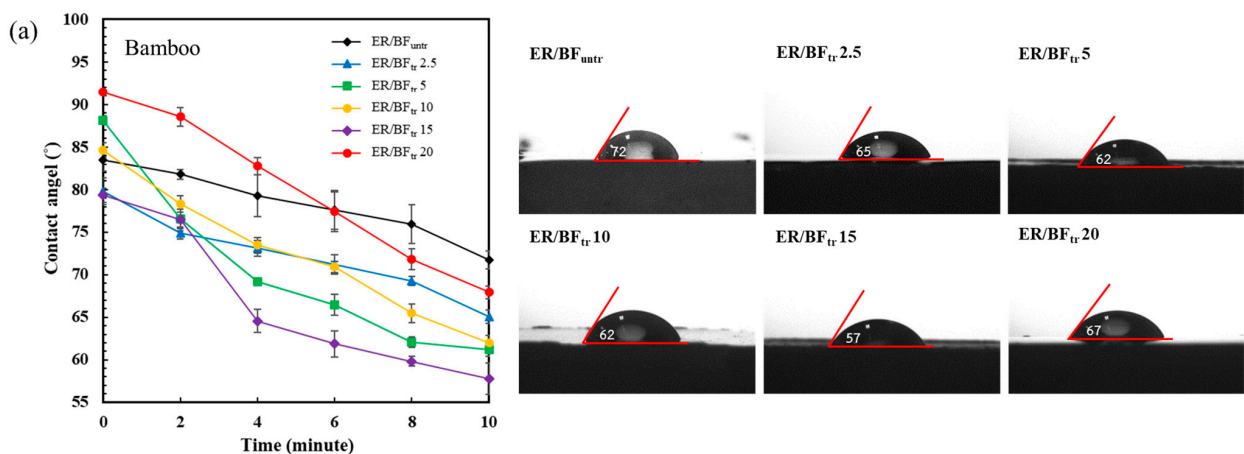


**Figure 6.** Cont.

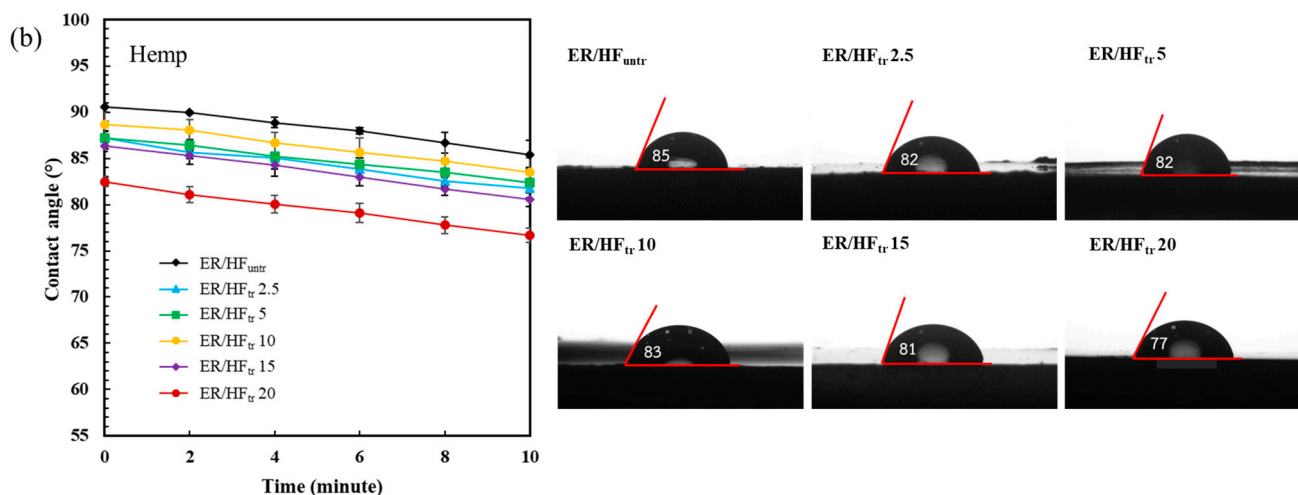


**Figure 6.** Water droplet contact angles and images of water contact angles at 10 min for the fiber-reinforced epoxy composites with untreated and plasma-treated structures: (a) BF and (b) HF.

#### 4. Conclusions

ER/BF and ER/HF were successfully developed with DBD Ar + O<sub>2</sub> plasma treatment. The Ar + O<sub>2</sub> gas plasma treatment significantly enhanced the properties of the bamboo and hemp fiber-reinforced epoxy composites. ER/BF<sub>tr</sub> was better in terms of tensile strength, while ER/HF<sub>tr</sub> exhibited a larger improvement in elongation at break. The FTIR spectroscopy confirmed the reaction between epoxy groups of ER with C–O and –NH<sub>2</sub> groups of the treated fibers, which improved the interfacial adhesion between the fiber surface and ER matrix. The ER/BF<sub>tr</sub> and ER/HF<sub>tr</sub> composites exhibited improved flexural strengths and flexural moduli after the Ar + O<sub>2</sub> plasma treatment due to the improved polarity and roughness of the fiber surface. The SEM analysis showed the fiber surface roughness with a low gap between fibers and ER matrix. The BFs exhibited a gradual increase in surface roughness with the treatment time, while the HFs exhibited a good interfacial adhesion with a low gap. The TGA also confirmed the improved thermal stability and reactions by the plasma treatment with a high weight loss for the long-term Ar + O<sub>2</sub> plasma treatment. The plasma treatment decreased the water contact angle owing to the increased content of hydrophilic groups, etching, porosity, and roughness of the fiber surface. The ER/BF<sub>tr</sub> and ER/HF<sub>tr</sub> composites can be employed in packaging, coating, construction, and electrical applications.

**Author Contributions:** K.J., P.W. (Pitiwat Wattanachai), C.S., and P.R. designed the research study; K.J., P.W. (Pitiwat Wattanachai), C.S., and P.R. methodology; P.R., P.W. (Pitiwat Wattanachai), C.S., P.W. (Patnarin Worajittiphon), J.S., N.T., and K.J. visualization, data analysis, and supervision; P.R., P.W. (Pitiwat Wattanachai), C.S., J.S., N.T., K.J., P.W. (Patnarin Worajittiphon), T.K., K.K., and P.T. prepared and investigated the samples; P.R., P.W. (Pitiwat Wattanachai), C.S., J.S., N.T., P.W. (Patnarin Worajittiphon), and K.J. discussed the results; K.J., T.K., P.W. (Pitiwat Wattanachai), C.S., and P.R. writing—original draft preparation. All authors have read and agreed to the published version of the manuscript.

**Funding:** This research has received funding support from the NSRF via the Program Management Unit for Human Resources and Institutional Development, Research, and Innovation (grant number B16F640206). This research work was partially supported by Chiang Mai University. The present study was partially supported by the Thailand Research Fund (TRF) Research Team Promotion Grant, RTA, Senior Research Scholar (N42A671052). This research and innovation activity was funded by the National Research Council of Thailand (NRCT) under the “Hub of Talents in Bioplastics for Use in Medical Applications” (Grant No. N34E670071).

**Institutional Review Board Statement:** Not applicable.

**Informed Consent Statement:** Not applicable.

**Data Availability Statement:** The data presented in this study are available upon request from the corresponding author.

**Acknowledgments:** This research work was partially supported by Chiang Mai University. The authors wish to express their sincere thanks to the Agriculture and Bio Plasma Technology Center (ABPlas), Science and Technology Park (STeP), and Faculty of Agro-industry, Chiang Mai University for laboratory equipment and resources support and the Center of Excellence in Materials Science and Technology, Chiang Mai University.

**Conflicts of Interest:** The authors declare no conflicts of interest.

### Abbreviations and Symbols

ER, epoxy resin; BF, bamboo fibers; HF, hemp fibers; DBD, dielectric barrier discharge; FTIR, Fourier-transform infrared spectroscopy; SEM, scanning electron microscopy; TGA, thermogravimetric analysis.

### References

1. Low, I.M.; McGrath, M.; Lawrence, D.; Schmidt, P.; Lane, J.; Latella, B.A.; Sim, K.S. Mechanical and fracture properties of cellulose-fibre-reinforced epoxy laminates. *Compos. A Appl. Sci. Manuf.* **2007**, *38*, 963–974. [[CrossRef](#)]
2. Shih, Y.-F. Mechanical and thermal properties of waste water bamboo husk fiber reinforced epoxy composites. *Mater. Sci. Eng. A* **2007**, *445–446*, 289–295. [[CrossRef](#)]
3. Gassan, J. Effects of corona discharge and UV treatment on the properties of jute-fibre epoxy composites. *Compos. Sci. Technol.* **2000**, *60*, 2857–2863. [[CrossRef](#)]
4. Radoor, S.; Karayil, J.; Rangappa, S.M.; Siengchin, S.; Parameswaranpillai, J. A review on the extraction of pineapple, sisal and abaca fibers and their use as reinforcement in polymer matrix. *Express Polym. Lett.* **2020**, *14*, 309–335. [[CrossRef](#)]
5. Ramadan, N.; Taha, M.; Elsabbagh, A. Processing and characterization of flame-retardant natural fibre-reinforced epoxy composites and construction of selection charts for engineering applications. *Express Polym. Lett.* **2024**, *18*, 779–795. [[CrossRef](#)]
6. Sukwijit, C.; Seubsai, A.; Charoenchaitrakool, M.; Sudsakorn, K.; Niamnuy, C.; Roddecha, S.; Prapainainar, P. Production of PLA/cellulose derived from pineapple leaves as bio-degradable mulch film. *Int. J. Biol. Macromol.* **2024**, *270*, 132299. [[CrossRef](#)] [[PubMed](#)]
7. Bachtiar, D.; Sapuan, S.M.; Hamdan, M.M. The effect of alkaline treatment on tensile properties of sugar palm fibre reinforced epoxy composites. *Mater. Des.* **2008**, *29*, 1285–1290. [[CrossRef](#)]
8. Alamri, H.; Low, I.M. Characterization of epoxy hybrid composites filled with cellulose fibers and nano-SiC. *J. Appl. Polym. Sci.* **2012**, *126*, E222–E232. [[CrossRef](#)]
9. Emamverdian, A.; Ding, Y.; Ranaei, F.; Ahmad, Z. Application of bamboo plants in nine aspects. *Sci. World J.* **2020**, *2020*, 7284203. [[CrossRef](#)]
10. Kiattipornpithak, K.; Rachtanapun, P.; Thanakkasaranee, S.; Jantrawut, P.; Ruksiriwanich, W.; Sommano, S.R.; Leksawasdi, N.; Kittikorn, T.; Jantanasakulwong, K. Bamboo pulp toughening poly (lactic acid) composite using reactive epoxy resin. *Polymers* **2023**, *15*, 3789. [[CrossRef](#)]
11. Huang, J.; Zhang, L.; Zhou, Y.; Huang, M.; Sha, Y. Study on the suitability of bamboo fiber for manufacturing insulating presspaper. *IEEE Trans. Dielectr. Electr. Insul.* **2016**, *23*, 3641–3651. [[CrossRef](#)]
12. Liu, D.; Song, J.; Anderson, D.P.; Chang, P.R.; Hua, Y. Bamboo fiber and its reinforced composites: Structure and properties. *Cellulose* **2012**, *19*, 1449–1480. [[CrossRef](#)]
13. Lokesh, P.; Surya Kumari, T.S.A.; Gopi, R.; Babu Loganathan, G. A study on mechanical properties of bamboo fiber reinforced polymer composite. *Mater. Today Proc.* **2020**, *22*, 897–903. [[CrossRef](#)]
14. Rohen, L.A.; Neves, A.C.C.; dos Santos, J.L.; Nascimento, L.F.C.; Monteiro, S.N.; de Assis, F.S.; Simonassi, N.T.; da Silva, L.C. Comparative analysis of the tensile properties of polyester and epoxy composites reinforced with hemp fibers. *Mater. Sci. Forum* **2018**, *930*, 201–206. [[CrossRef](#)]
15. Islam, M.S.; Pickering, K.L.; Foreman, N.J. Influence of alkali fiber treatment and fiber processing on the mechanical properties of hemp/epoxy composites. *J. Appl. Polym. Sci.* **2010**, *119*, 3696–3707. [[CrossRef](#)]
16. Valadez-Gonzalez, A.; Cervantes-Uc, J.M.; Olayo, R.; Herrera-Franco, P.J. Effect of fiber surface treatment on the fiber–matrix bond strength of natural fiber reinforced composites. *Compos. B Eng.* **1999**, *30*, 309–320. [[CrossRef](#)]
17. Thipchai, P.; Punyodom, W.; Jantanasakulwong, K.; Thanakkasaranee, S.; Hinmo, S.; Pratinthong, K.; Kasi, G.; Rachtanapun, P. Preparation and characterization of cellulose nanocrystals from bamboos and their application in cassava starch-based film. *Polymers* **2023**, *15*, 2622. [[CrossRef](#)]
18. Suriyatem, R.; Noikang, N.; Kankam, T.; Jantanasakulwong, K.; Leksawasdi, N.; Phimolsiripol, Y.; Insomphun, C.; Seesuriyachan, P.; Chaiyaso, T.; Jantrawut, P.; et al. Physical properties of carboxymethyl cellulose from palm bunch and bagasse agricultural wastes: Effect of delignification with hydrogen peroxide. *Polymers* **2020**, *12*, 1505. [[CrossRef](#)] [[PubMed](#)]

19. Zhou, F.; Cheng, G.; Jiang, B. Effect of silane treatment on microstructure of sisal fibers. *Appl. Surf. Sci.* **2014**, *292*, 806–812. [[CrossRef](#)]
20. Xie, J.; Xin, D.; Cao, H.; Wang, C.; Zhao, Y.; Yao, L.; Ji, F.; Qiu, Y. Improving carbon fiber adhesion to polyimide with atmospheric pressure plasma treatment. *Surf. Coat. Technol.* **2011**, *206*, 191–201. [[CrossRef](#)]
21. Karaduman, Y.; Gokcan, D.; Onal, L. Effect of enzymatic pretreatment on the mechanical properties of jute fiber-reinforced polyester composites. *J. Compos. Mater.* **2012**, *47*, 1293–1302. [[CrossRef](#)]
22. Oliveira, F.R.; Erkens, L.; Figueiro, R.; Souto, A.P. Surface modification of banana fibers by DBD plasma treatment. *Plasma Chem. Plasma Process.* **2012**, *32*, 259–273. [[CrossRef](#)]
23. Phan, K.T.K.; Phan, H.T.; Brennan, C.S.; Regenstein, J.M.; Jantanasakulwong, K.; Boonyawan, D.; Phimolsiripol, Y. Gliding arc discharge non-thermal plasma for retardation of mango anthracnose. *LWT* **2019**, *105*, 142–148. [[CrossRef](#)]
24. Faruk, O.; Bledzki, A.K.; Fink, H.-P.; Sain, M. Progress report on natural fiber reinforced composites. *Macromol. Mater. Eng.* **2014**, *299*, 9–26. [[CrossRef](#)]
25. Peças, P.; Carvalho, H.; Salman, H.; Leite, M. Natural fibre composites and their applications: A Review. *J. Compos. Sci.* **2018**, *2*, 66. [[CrossRef](#)]
26. Liston, E.M. Plasma treatment for improved bonding: A Review. *J. Adhes.* **1989**, *30*, 199–218. [[CrossRef](#)]
27. Sawangrat, C.; Thipchai, P.; Kaewapai, K.; Jantanasakulwong, K.; Suhr, J.; Wattanachai, P.; Rachtanapun, P. Surface modification and mechanical properties improvement of bamboo fibers using dielectric barrier discharge plasma treatment. *Polymers* **2023**, *15*, 1711. [[CrossRef](#)]
28. Rachtanapun, P.; Sawangrat, C.; Kanthiya, T.; Thipchai, P.; Kaewapai, K.; Suhr, J.; Worajittiphon, P.; Tanadchangsang, N.; Wattanachai, P.; Jantanasakulwong, K. Effect of plasma treatment on bamboo fiber-reinforced epoxy composites. *Polymers* **2024**, *16*, 938. [[CrossRef](#)] [[PubMed](#)]
29. Lee, D.; Hong, S.H.; Paek, K.-H.; Ju, W.-T. Adsorbability enhancement of activated carbon by dielectric barrier discharge plasma treatment. *Surf. Coat. Technol.* **2005**, *200*, 2277–2282. [[CrossRef](#)]
30. Biswas, S.; Shahinur, S.; Hasan, M.; Ahsan, Q. Physical, mechanical and thermal properties of jute and bamboo fiber reinforced unidirectional epoxy composites. *Procedia Eng.* **2015**, *105*, 933–939. [[CrossRef](#)]
31. Mashouf Roudsari, G.; Mohanty, A.K.; Misra, M. Study of the curing kinetics of epoxy resins with biobased hardener and epoxidized soybean oil. *ACS Sustain. Chem. Eng.* **2014**, *2*, 2111–2116. [[CrossRef](#)]
32. Uflyand, I.E.; Irzhak, V.I. Recent advances in the study of structure and properties of fiber composites with an epoxy matrix. *J. Polym. Res.* **2021**, *28*, 440. [[CrossRef](#)]
33. Mohan, P. A Critical Review: The modification, properties, and applications of epoxy resins. *Polym. Plast. Technol. Eng.* **2013**, *52*, 107–125. [[CrossRef](#)]
34. Kodsangma, A.; Homsaard, N.; Nadon, S.; Rachtanapun, P.; Leksawasdi, N.; Phimolsiripol, Y.; Insomphun, C.; Seesuriyachan, P.; Chaiyaso, T.; Jantrawut, P.; et al. Effect of sodium benzoate and chlorhexidine gluconate on a bio-thermoplastic elastomer made from thermoplastic starch-chitosan blended with epoxidized natural rubber. *Carbohydr. Polym.* **2020**, *242*, 116421. [[CrossRef](#)]
35. Ma, H.; Whan Joo, C. Influence of surface treatments on structural and mechanical properties of bamboo fiber-reinforced poly(lactic acid) biocomposites. *J. Compos. Mater.* **2011**, *45*, 2455–2463. [[CrossRef](#)]
36. Sgriccia, N.; Hawley, M.C.; Misra, M. Characterization of natural fiber surfaces and natural fiber composites. *Compos. A Appl. Sci. Manuf.* **2008**, *39*, 1632–1637. [[CrossRef](#)]
37. Bozaci, E.; Sever, K.; Sarikanat, M.; Seki, Y.; Demir, A.; Ozdogan, E.; Tavman, I. Effects of the atmospheric plasma treatments on surface and mechanical properties of flax fiber and adhesion between fiber–matrix for composite materials. *Compos. B Eng.* **2013**, *45*, 565–572. [[CrossRef](#)]
38. Rayung, M.; Ibrahim, N.A.; Zainuddin, N.; Saad, W.Z.; Razak, N.I.; Chieng, B.W. The effect of fiber bleaching treatment on the properties of poly(lactic acid)/oil palm empty fruit bunch fiber composites. *Int. J. Mol. Sci.* **2014**, *15*, 14728–14742. [[CrossRef](#)]
39. Liu, W.; Mohanty, A.K.; Drzal, L.T.; Askel, P.; Misra, M. Effects of alkali treatment on the structure, morphology and thermal properties of native grass fibers as reinforcements for polymer matrix composites. *J. Mater. Sci.* **2004**, *39*, 1051–1054. [[CrossRef](#)]
40. Kiatipornpipthak, K.; Thajai, N.; Kanthiya, T.; Rachtanapun, P.; Leksawasdi, N.; Phimolsiripol, Y.; Rohindra, D.; Ruksiriwanich, W.; Sommano, S.R.; Jantanasakulwong, K. Reaction mechanism and mechanical property improvement of poly(lactic acid) reactive blending with epoxy resin. *Polymers* **2021**, *13*, 2429. [[CrossRef](#)]
41. Dimitrakellis, P.; Faubert, F.; Wartel, M.; Gogolides, E.; Pellerin, S. Plasma surface modification of epoxy polymer in air DBD and gliding arc. *Processes* **2022**, *10*, 104. [[CrossRef](#)]
42. Kanthiya, T.; Kiatipornpipthak, K.; Thajai, N.; Phimolsiripol, Y.; Rachtanapun, P.; Thanakkasarnanee, S.; Leksawasdi, N.; Tanadchangsang, N.; Sawangrat, C.; Wattanachai, P.; et al. Modified poly(lactic acid) epoxy resin using chitosan for reactive blending with epoxidized natural rubber: Analysis of annealing time. *Polymers* **2022**, *14*, 1085. [[CrossRef](#)] [[PubMed](#)]
43. Baghery Borooj, M.; Mousavi Shoushtari, A.; Nosratian Sabet, E.; Haji, A. Influence of oxygen plasma treatment parameters on the properties of carbon fiber. *J. Adhes. Sci. Technol.* **2016**, *30*, 2372–2382. [[CrossRef](#)]
44. Pitto, M.; Fiedler, H.; Kim, N.K.; Verbeek, C.J.R.; Allen, T.D.; Bickerton, S. Carbon fibre surface modification by plasma for enhanced polymeric composite performance: A review. *Compos. Part A* **2024**, *180*, 108087. [[CrossRef](#)]

45. Kanthiya, T.; Thajai, N.; Chaiyaso, T.; Rachtanapun, P.; Thanakkasaranee, S.; Kumar, A.; Boonrasri, S.; Kittikorn, T.; Phimolsiripol, Y.; Leksawasdi, N.; et al. Enhancement in mechanical and antimicrobial properties of epoxidized natural rubber via reactive blending with chlorhexidine gluconate. *Sci. Rep.* **2023**, *13*, 9974. [[CrossRef](#)]
46. Manjula, S.; Shanmugasundaram, O.L.; Ponappa, K. Optimization of plasma process parameters for surface modification of bamboo spunlace nonwoven fabric using glow discharge oxygen plasma. *J. Ind. Text.* **2019**, *51*, 225–245. [[CrossRef](#)]
47. Sánchez, M.L.; Patiño, W.; Cárdenas, J. Physical-mechanical properties of bamboo fibers-reinforced biocomposites: Influence of surface treatment of fibers. *J. Build. Eng.* **2020**, *28*, 101058. [[CrossRef](#)]
48. Li, S.; Han, K.; Rong, H.; Li, X.; Yu, M. Surface modification of aramid fibers via ammonia-plasma treatment. *J. Appl. Polym. Sci.* **2013**, *131*, 40250. [[CrossRef](#)]
49. Mohit, H.; Arul Mozhi Selvan, V. A comprehensive review on surface modification, structure interface and bonding mechanism of plant cellulose fiber reinforced polymer-based composites. *Compos. Interfaces* **2018**, *25*, 629–667. [[CrossRef](#)]
50. Chen, Y.; Xu, C.; Wang, C.H.; Bilek, M.M.M.; Cheng, X. An effective method to optimise plasma immersion ion implantation: Sensitivity analysis and design based on low-density polyethylene. *Plasma Process. Polym.* **2022**, *19*, e2100199. [[CrossRef](#)]
51. Kim, S.Y.; Hong, K.; Kim, K.; Yu, H.K.; Kim, W.-K.; Lee, J.-L. Effect of N<sub>2</sub>, Ar, and O<sub>2</sub> plasma treatments on surface properties of metals. *J. Appl. Phys.* **2008**, *103*, 076101. [[CrossRef](#)]
52. Pejic, B.M.; Kramar, A.D.; Obradovic, B.M.; Kuraica, M.M.; Zekic, A.A.; Kostic, M.M. Effect of plasma treatment on chemical composition, structure and sorption properties of lignocellulosic hemp fibers (*Cannabis sativa* L.). *Carbohydr. Polym.* **2020**, *236*, 116000. [[CrossRef](#)]
53. Ivanovska, A.; Milošević, M.; Obradović, B.; Svirčev, Z.; Kostić, M. Plasma treatment as a sustainable method for enhancing the wettability of jute fabrics. *Sustainability* **2023**, *15*, 2125. [[CrossRef](#)]
54. Ren, Z.; Tang, X.; Wang, H.; Qiu, G. Continuous modification treatment of polyester fabric by Ar-O<sub>2</sub>(10:1) Discharge at atmospheric pressure. *J. Ind. Text.* **2016**, *37*, 43–53.
55. Zhang, D.; Huang, Y. Dispersion characterizations and adhesion properties of epoxy composites reinforced by carboxymethyl cellulose surface treated carbon nanotubes. *Powder Technol.* **2022**, *404*, 117505. [[CrossRef](#)]
56. Zhang, D.; Huang, Y.; Xia, W.; Xu, L.; Wang, X. Dispersion characteristics and mechanical properties of epoxy nanocomposites reinforced with carboxymethyl cellulose functionalized nanodiamond, carbon nanotube, and graphene. *Polym. Compos.* **2023**, *45*, 398–412. [[CrossRef](#)]
57. Movahed, S.; Nguyen, A.K.; Goering, P.L.; Skoog, S.A.; Narayan, R.J. Argon and oxygen plasma treatment increases hydrophilicity and reduces adhesion of silicon-incorporated diamond-like coatings. *Biointerphases* **2020**, *15*, 041007. [[CrossRef](#)] [[PubMed](#)]
58. Kan, C.W.; Chan, K.; Yuen, C.W.M. Surface characterization of low temperature plasma treated wool fiber. *Fibers Polym.* **2004**, *5*, 52–58. [[CrossRef](#)]
59. Marrot, L.; Lefeuvre, A.; Pontoire, B.; Bourmaud, A.; Baley, C. Analysis of the hemp fiber mechanical properties and their scattering (Fedora 17). *Ind. Crops Prod.* **2013**, *51*, 317–327. [[CrossRef](#)]
60. Relvas, C.; Castro, G.; Rana, S.; Fangueiro, R. characterization of physical, mechanical and chemical properties of Quiscal Fibres: The influence of atmospheric DBD plasma treatment. *Plasma Chem. Plasma Process.* **2015**, *35*, 863–878. [[CrossRef](#)]
61. Alonso-Montemayor, F.J.; López-Badillo, C.M.; Aguilar, C.N.; Ávalos-Belmontes, F.; Castañeda-Facio, A.O.; Reyna-Martínez, R.; Neira-Velázquez, M.G.; Soria-Argüello, G.; Navarro-Rodríguez, D.; Delgado-Aguilar, M.; et al. Effect of cold air plasmas on the morphology and thermal stability of bleached hemp fibers. *Rev. Mex. Ing. Quim.* **2020**, *19*, 457–467. [[CrossRef](#)]
62. Silva, T.T.D.; Silveira, P.; Ribeiro, M.P.; Lemos, M.F.; da Silva, A.P.; Monteiro, S.N.; Nascimento, L.F.C. Thermal and chemical characterization of kenaf fiber (*Hibiscus cannabinus*) reinforced epoxy matrix composites. *Polymers* **2021**, *13*, 2016. [[CrossRef](#)] [[PubMed](#)]
63. Misnon, M.I.; Islam, M.M.; Epaarachchi, J.A.; Lau, K.T. Analyses of woven hemp fabric characteristics for composite reinforcement. *Mater. Des.* **2015**, *66*, 82–92. [[CrossRef](#)]
64. Scalici, T.; Fiore, V.; Valenza, A. Effect of plasma treatment on the properties of *Arundo Donax* L. leaf fibres and its bio-based epoxy composites: A preliminary study. *Compos. B Eng.* **2016**, *94*, 167–175. [[CrossRef](#)]
65. Mohammed, Z.; Jeelani, S.; Rangari, V.K. Effect of low-temperature plasma treatment on starch-based biochar and its reinforcement for three-dimensional printed polypropylene biocomposites. *ACS Omega* **2022**, *7*, 39636–39647. [[CrossRef](#)]
66. Lieberman, M.A.; Lichtenberg, A.J. Principles of Plasma Discharges and Materials Processing. *MRS Bull.* **2005**, *30*, 899.
67. Tan, S.H.; Nguyen, N.T.; Chua, Y.C.; Kang, T.G. Oxygen plasma treatment for reducing hydrophobicity of a sealed polydimethylsiloxane microchannel. *Biomicrofluidics* **2010**, *4*, 32204. [[CrossRef](#)]

**Disclaimer/Publisher's Note:** The statements, opinions and data contained in all publications are solely those of the individual author(s) and contributor(s) and not of MDPI and/or the editor(s). MDPI and/or the editor(s) disclaim responsibility for any injury to people or property resulting from any ideas, methods, instructions or products referred to in the content.